



Comments and Controversies

On determining the intracranial sources of visual evoked potentials from scalp topography: A reply to Kelly et al. (this issue)

Justin M. Ales^{a,*}, Jacob L. Yates^b, Anthony M. Norcia^a^a Department of Psychology, Stanford University, Stanford, CA, USA^b The Institute for Neuroscience, University of Texas at Austin, Austin, TX, USA

ARTICLE INFO

Article history:

Accepted 5 September 2012

Available online 13 September 2012

Keywords:

Evoked potentials

C1

Cruciform model

V1

EEG

fMRI

ABSTRACT

The cruciform model posits that if a Visual Evoked Potential component originates in cortical area V1, then stimuli placed in the upper versus lower visual field will generate responses with opposite polarity at the scalp. In our original paper (Ales et al., 2010b) we showed that the cruciform model provides an insufficient criterion for identifying V1 sources. This conclusion was reached on the basis of simulations that used realistic 3D models of early visual areas to simulate scalp topographies expected for stimuli of different sizes and shapes placed in different field locations. The simulations indicated that stimuli placed in the upper and lower visual field produce polarity inverting scalp topographies for activation of areas V2 and V3, but not for area V1. As a consequence of the non-uniqueness of the polarity inversion criterion, we suggested that past studies using the cruciform model had not adequately excluded contributions from sources outside V1. In their comment on our paper, Kelly et al. (this issue) raise several concerns with this suggestion. They claim that our initial results did not use the proper stimulus locations to constitute a valid test of the cruciform model. Kelly et al., also contend that the cortical source of the initial visually evoked component (C1) can be identified based on latency and polarity criteria derived from intracranial recordings in non-human primates. In our reply we show that simulations using the suggested critical stimulus locations are consistent with our original findings and thus do not change our conclusions regarding the use of the polarity inversion criterion. We further show that the anatomical assumptions underlying the putatively optimal locations are not consistent with available V1 anatomical data. We then address the non-human primate data, describing how differences in stimuli across studies and species confound an effective utilization of the non-human primate data for interpreting human evoked potential responses. We also show that, considered more broadly, the non-human primate literature shows that multiple visual areas onset simultaneously with V1. We suggest several directions for future research that will further clarify how to make the best use of scalp data for inferring cortical sources.

© 2012 Elsevier Inc. All rights reserved.

Introduction

Prior work has suggested that response polarity inversion for upper and lower visual field stimuli can be used isolate the response generated by cortical area V1 (Jeffreys, 1971; Jeffreys and Axford, 1972a). The underlying geometric model on which this technique is based has come to be known as “the cruciform model.” Ales et al. (2010b) used measurements of the 3-D geometry of visual areas V1, V2 and V3 to simulate the scalp topographies for stimuli placed in the lower and upper visual fields. In our original paper, we showed that simulated upper and lower field sources in V1 did not produce frank polarity inversions at the scalp, but that sources in V2 and V3 did. Because of this result, we suggested that the Event-Related

Potential (ERP) component C1, which shows such polarity inversions, might not reflect responses arising solely from cortical area V1. Kelly et al. (this issue) were critical of this suggestion for several reasons. We thank Kelly et al. (this issue) for their comments that have prompted us to clarify our initial claims and to more fully address this important issue.

Kelly et al. (this issue) raised several concerns that we will address in four parts. First, Kelly et al. (this issue) state that we failed to perform a critical simulation and thus what we presented did not adequately address predictions from prior work (Clark et al., 1995; Di Russo et al., 2002). Kelly et al. (this issue) made a specific suggestion for the proper simulation. In Section “Simulations of scalp topographies generated by nominally optimal stimulus locations”, we present results from the simulation suggested by Kelly et al. (this issue). These results show that even for putatively optimal stimulus locations, fields generated by V1 sources do not fully polarity invert at the scalp, but those from V2 and V3 do.

* Corresponding author.

E-mail addresses: justin.ales@stanford.edu, justin.ales@gmail.com (J.M. Ales).

Kelly et al. (this issue) suggested that the true shape and visual field topography of V1 reflects the model of V1 presented in (Clark et al., 1995). In Section “Origins and validity of cruciform models”, we review the 3D anatomy of striate and extra-striate cortex and the location of the horizontal meridian predicted by the revised cruciform model (Clark et al., 1995). We find that a main prediction of the revised cruciform model—that the horizontal meridian in V1 is shifted away from the fundus of the calcarine sulcus—has no independent support in the anatomical literature.

Kelly et al. (this issue) state that even if the human anatomy fails to support the cruciform model, it is still possible to identify V1 sources on the basis of the relative timing of V1 evoked responses that have been derived from primate intracranial recordings. In Section “Response timing and comparisons with intracranially recorded data”, we review the non-human primate evidence for significant time delays between V1 and the rest of the visual hierarchy and conclude that the available evidence does not support a clear and substantial time window during which V1 is active in isolation. Finally, in Section “Interpreting C1 in human studies”, we review human ERP evidence that is consistent with the presence of substantial extra-striate contributions to the C1 component measured at the scalp.

Simulations of scalp topographies generated by nominally optimal stimulus locations

Kelly et al. (this issue) state that we inappropriately truncated the complete form of the cruciform model in our cartoon depiction of the model and that our simulations used stimuli that were too large and that were not placed at optimal locations. Kelly et al. (this issue) suggest that the correct way to test the revised cruciform model would be to simulate responses from a set of optimal visual field locations for isolating V1 activity via a polarity inversion at the scalp for upper vs. lower field responses.

Fig. 1 shows the result of the simulation suggested by Kelly et al. (this issue). We simulated topographies for the first 10 of our original subjects for a 1° radius circle centered 4° from fixation, angled +25° and −45° from the horizontal meridian. These correspond to the polar angles determined by Clark et al. (1995) and these stimulus locations have been used to study the sources of evoked potentials (Di Russo et al., 2002, 2005). We used identical methodology to Ales et al. (2010b). Briefly, we used retinotopic maps provided by fMRI and MRI to define the location and orientation of the sources corresponding to the visual stimuli. We then calculated the topographies for these stimulus locations in each subject, and then averaged

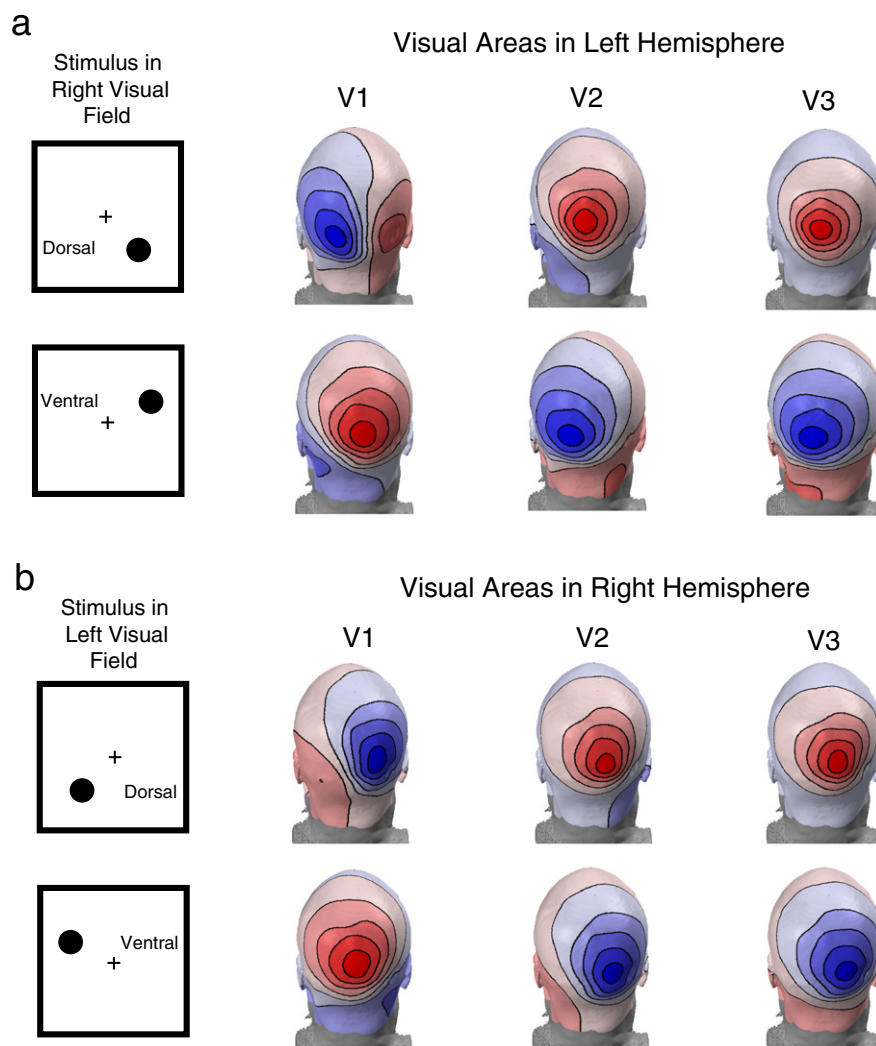


Fig. 1. Scalp topographies for the stimulus locations suggested by Kelly et al. (this issue) averaged over 10 subjects. Methods for generating these topographies are identical to Ales et al. (2010b). Each color map is scaled separately to highlight the shape of the topography, with red colors representing positive potentials, and blue colors representing negative potentials. a) Simulations for right visual field. b) Simulations for left visual field.

these topographies at the electrodes across the subjects. Finally, we plotted this average topography on a realistic scalp surface.

The new results are in accordance with our previous findings (Ales et al., 2010b). Fig. 2 collects the three different stimulus shapes we have simulated. The topographies for the optimal locations are most similar to the previous results for 3–4° ring stimuli. One-degree radius circles suggested by Kelly et al. (this issue) produce topographies for extrastriate areas V2 and V3 that are similar to our previous results from rings that spanned an entire quadrant. The proposed optimal stimulus locations suggested by Kelly et al. (this issue) for isolating V1 do not generate a full polarity inversion for sources in V1. However, areas V2 and V3 do produce topographies that are almost completely polarity inverted on an electrode-by-electrode basis for stimuli in the

upper and lower visual fields for the nominally optimal stimulus parameters suggested. The lack of polarity inversion for V1 sources in our original report was not due to a failure of simulating the critical stimulus values needed to elicit a polarity inversion in V1.

Origins and validity of cruciform models

Given the failure of nominally optimal stimulus locations to produce the predicted “clear polarity inversion” for V1 sources, combined with the fact that V2 and V3 sources do, it is instructive to delve into the origins of the original cruciform model and its more recent variant. Jeffreys (1969, 1971) introduced the idea that the orderly arrangement of retinotopic cortex enables one to choose appropriate stimuli that

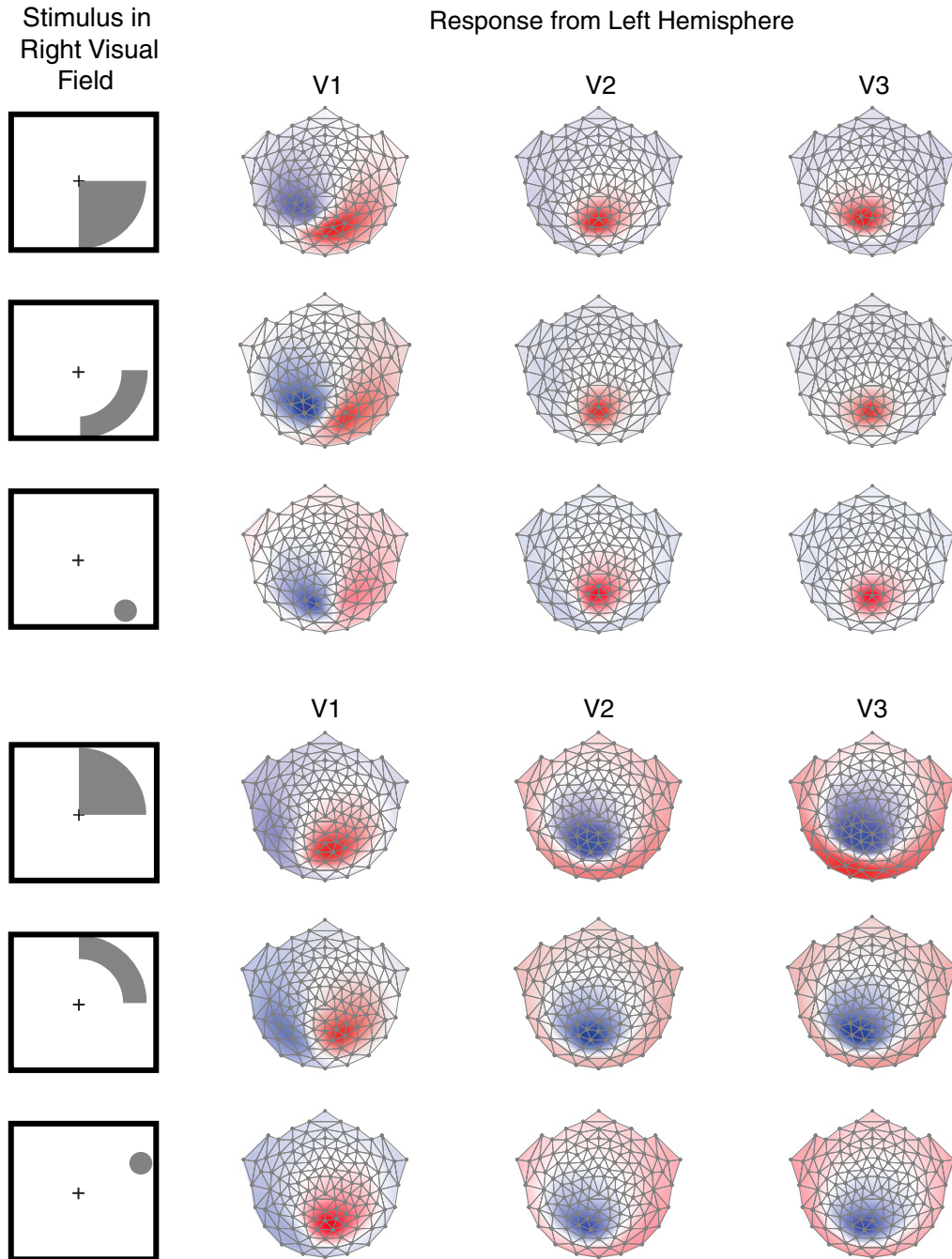


Fig. 2. Scalp topographies generated by different retinotopic stimulus locations. Each color map is scaled separately to highlight the shape of the topography, with red colors representing positive potentials, and blue colors representing negative potentials. Changing the stimulus configuration has the largest effect on topographies from V1, with minor changes to topographies from V2 and V3.

distinguish between striate and extrastriate generators of scalp VEP's. [Jeffreys and Axford \(1972a,b\)](#) went on to systematically investigate the correlation between stimulus locations and human VEP responses. At the time of their studies, however, Jeffreys & Axford had to rely on data from clinical examinations of the visual field defects caused by World War I gunshot wounds ([Holmes, 1945](#)). Besides a verbal description, [Holmes \(1945\)](#) provided a hand-drawn annotation of the location of visual areas on a cadaver brain. What was available at the time of the original formulation of the cruciform model was thus highly schematic.

The 3D geometry of striate cortex

[Clark et al. \(1995\)](#) revised the original Jeffreys & Axford model on the basis of inferences they made about shape of striate cortex that were based on the scalp topography of VEP responses and dipole modeling. [Clark et al. \(1995\)](#) presented small stimuli at many locations in the upper and lower visual fields at 8° eccentricity. Based on recordings made with these stimuli, the entire set of topographic data from 50 to 80 ms was fit with two dipoles (P1 and C1), both of whose locations were fixed, with the P1 dipole's orientation also fixed. Only the C1 dipole's orientation was free to vary. Fixing the orientation of the P1 source effectively contaminates the estimate of the orientation of the C1 source. The orientation of the C1 source must account for both the changing orientation of V1 and also the changing orientation of extrastriate sources. The orientation of this C1 dipole was then used to estimate the surface normals of a pre-specified, cruciform-shaped V1 (see Figure 11 of [Clark et al., 1995](#)). Based on this assumed shape for V1, [Clark et al. \(1995\)](#) needed to move the location of the horizontal meridian away from the fundus of the calcarine sulcus to a location on the ventral bank. This was forced because the VEP inverted polarity for stimuli presented 20° below the horizontal meridian. Several other VEP and MEG studies have also found that scalp polarities do not invert at the horizontal meridian ([Aine et al., 1996](#); [James, 2003](#); [Zhang and Hood, 2004](#)). In supporting this revision, [Clark et al. \(1995\)](#) claimed that [Spalding \(1952\)](#), a study of visual field defects after gunshot wounds, found that the horizontal meridian was represented ventrally. However, this is a misinterpretation of Spalding's findings. [Spalding \(1952, page 181\)](#) stated that the horizontal meridian was represented on the "floor" of the calcarine sulcus and used the term floor to mean the fundus of the calcarine sulcus and the term "walls" to mean the banks of the sulcus.

[Clark et al.'s \(1995\)](#) revision of the location of the horizontal meridian based on surface VEP measurements is not supported by any direct anatomical measurement. [Kelly et al. \(this issue\)](#) argue that histological data are highly consistent with the horizontal meridian being shifted from the fundus of the calcarine sulcus. Histological analysis does not provide the location of the horizontal meridian. Histological data can only define the location of the vertical meridian, via the stripe of Gennari. One simply cannot use the locations of the vertical meridians of V1 to locate the horizontal meridian within the sulcus. What is needed is a methodology that directly links the visually defined horizontal meridian to the anatomically defined calcarine sulcus. Existing data of this type is consistent with striate cortex folding precisely along the horizontal meridian. Studies of the sources of visual field defects that were correlated with MRI findings ([Galletta and Grossman, 2000](#); [Gray et al., 1998](#); [Horton and Hoyt, 1991](#); [McFadzean et al., 1994](#); [McFadzean and Hadley, 1997](#)) each state that the horizontal meridian is located at the fundus of the calcarine.

A recent fMRI study ([Rajimehr and Tootell, 2009](#)) found that meridian representations correlate with the curvature of cortex, with horizontal meridians located in sulci, and vertical meridians on gyri. The functional MRI data of [Rajimehr and Tootell \(2009\)](#) are consistent with the field defect studies, but the use of 45° wedges for mapping resulted in insufficient resolution to conclusively rule out a 20° shift. Surprisingly, no study has yet quantified the uncertainty of the location of the horizontal meridian in the calcarine sulcus. FMRI measurements

with very thin wedges, such as those used by [Bridge et al. \(2005\)](#) to map the vertical meridian, could definitively locate the horizontal meridian with respect to the fundus in living brains. These data would be useful more broadly because the precise location of the horizontal meridian at the fundus of the sulcus is the basis of an important computational model of the development of cortical folding ([Van Essen, 1997](#)). The model hypothesizes that the calcarine sulcus folds at the horizontal meridian in order to minimize the distance axons have to travel between equivalent retinotopic locations in different visual areas. A shifted meridian would force a reconsideration of the folding model.

The revised cruciform model also postulates that much of striate cortex lies outside the calcarine sulcus ([Aine et al., 1996](#)). It is true that boundaries of striate cortex are outside of the calcarine sulcus. The main concern was that our original simulations, by extending to the vertical meridians, included too much cortex outside of the calcarine sulcus. We addressed this issue in Section "Simulations of scalp topographies generated by nominally optimal stimulus locations" by simulating smaller retinotopically defined sources. These smaller sources produced different topographies from sources in V1, but did not generate a polarity inverting V1 source. While the size of our previously simulated stimuli is a valid criticism, it is not as large a problem as was suggested. The revised cruciform model claims that a much larger proportion of striate cortex is outside of the sulcus than is consistent with anatomical data. [Kelly et al. \(this issue\)](#) state "the full primary visual cortical area extends as much outside the calcarine sulcus as inside". This statement is inconsistent with fMRI data and anatomical mapping data. FMRI data reveal that area V1 extends just beyond the lip of the calcarine. This can be seen by comparing V1 and V2 locations on the cortical surface in Figure 2 of [Fischl et al. \(2008\)](#) and Figure 3 of [Wilms et al. \(2010\)](#), as well as the location of V1 shown in Figure 2 of [Hinds et al. \(2008a\)](#). [Horton and Hoyt \(1991\)](#) provide a summary drawing of the location of V1 from their reconstructions of this area based on field defects. It shows very little of V1 exposed on the medial surface. However, there is some confusion in the literature about exactly how much of striate cortex is restricted to the calcarine fissure. [Stensaas et al. \(1974\)](#) quantified the amount of exposed striate cortex and their results have been interpreted to indicate that either 55% ([Aine et al., 1996](#)) or 67% ([Hinds et al., 2008b](#)) of V1 is buried within the calcarine sulcus. In addition, [Spalding \(1952, page 181\)](#) states "the walls and floor of the calcarine fissure represent two thirds of the visual field". These data argue that the majority of striate cortex (~67%) is inside the calcarine sulcus, with only ~33% outside the sulcus.

Even though the revised cruciform model does not match the existing anatomical data on striate cortex, the differences are nuanced and the anatomical studies have unspecified resolution. Studies of field defects following lesions cannot quantify shifts of a few degrees of polar angle. Most fMRI studies have identified the borders between different visual areas based on meridian locations, usually on flattened representations of cortex, but have not provided the detailed 3-D locations of the location of the V1 horizontal meridian. The discrepancies between the shape inferred from C1 orientation changes and the shape found in anatomical studies would be best resolved by specific targeted research. Answering this question has relevance beyond addressing the neural generators of the VEP, as the shape and topography of striate cortex is of fundamental importance to understanding not only EEG topographies, but also visual field defects and models of cortical connectivity and development.

The orientation of extrastriate sources

In our study, we found that simulated activation of extrastriate areas V2 and V3 produces polarity inversions for upper and lower field stimuli. [Kelly et al. \(this issue\)](#) state that our finding of a polarity inversion in V2 and V3 is "wholly unsurprising". We agree, and note here that while [Foxy and Simpson \(2002\)](#) made this observation before us, the point has not been made by most other studies. [Kelly et al. \(this issue\)](#)

state that [Jeffreys and Axford \(1972b\)](#) found that CII showed a polarity inversion for upper vs. lower field stimuli ([Figs. 2 and 3](#)) and that our main finding of polarity inversion for extrastriate sources “is not at all contrary to [Jeffreys & Axford]’s model”. However, this is inconsistent with Jeffreys and Axford’s own interpretation. [Jeffreys and Axford \(1972b\)](#) modeled their measured topographies with orthogonally, and not oppositely, oriented dipoles for the upper and lower fields. Jeffreys and Axford state “the equivalent dipole sources for the extrastriate cortical regions representing the upper and lower half-fields will be roughly perpendicular as shown in Fig. 8”. ([Jeffreys and Axford, 1972b, page 32](#)). In many studies, the assumptions made about the orientation of extrastriate sources have not been stated explicitly. It is our opinion that researchers have ignored the problem of polarity inverting extrastriate sources. The following quote is one such example:

“At a given eccentricity, a stimulus patch in the upper visual field and a stimulus patch in the lower visual field are expected to activate the lower and upper bank of the calcarine sulcus respectively. The corresponding dipoles are expected to reverse in polarity. This reversal is characteristic of the primary visual cortex and serves as a means to identify signals from this source.” ([Slotnick et al., 1999](#))

It is important for researchers to recognize that polarity inversions are not unique to sources in striate cortex. Because polarity inversions are not unique, they do not serve to exclude V2 and/or V3. Without clearly excluding V2 and V3, it becomes impossible to decide whether a response change from an experimental manipulation is a manifestation of the modulation of responses in V1, V2, or V3.

Response timing and comparisons with intracranially recorded data

[Kelly et al. \(this issue\)](#) note

“...even if stronger polarity inversion were demonstrated for extrastriate cortex compared to striate cortex for those parameters, how much of a problem would it present to the tenet that C1 is generated in V1? It stands to reason that the relative response latency, relative response strength, and the polarity, of the initial afferent potentials on the cortical surface in V1, V2 and V3 are critical factors. Fortunately, there exist extensive data on these factors, owing to intracranial recordings in non-human primates.”

There have, in fact, been relatively few studies that have compared evoked response latencies in different cortical areas for the same stimuli and even fewer that have compared latencies across areas for stimuli that are typically used to evoke a C1 response. Across human and primate studies, a wide range of stimuli have been used, from brief, large, diffuse flashes ([Schroeder et al., 1992](#)), to small pattern reversing checkerboards ([Ales et al., 2010a; Di Russo et al., 2005](#)), to stimuli independently optimized for isolated single-units ([Schmolesky et al., 1998](#)). Because different stimuli evoke responses with different component morphology and latency ([Odom et al., 2009; Schroeder et al., 1991](#)), it can be difficult to directly compare across studies. Below we will review the available intracranial data and demonstrate that the evidence for C1 being generated solely by V1 is equivocal.

Onset latencies of visual areas

[Kelly et al. \(this issue\)](#) claim that it is well established that there is a significant latency offset across ascending stages of the visual pathway, with V1 being activated first and in isolation. As evidence for this claim they cite a series of macaque studies ([Chen et al., 2007; Givre et al., 1994; Givre et al., 1995; Maunsell and Gibson, 1992; Nowak et al., 1999; Raiguel et al., 1989; Schmolesky et al., 1998; Schroeder et al., 1998, 2004](#)) stating that all of these studies “... agree on the presence of significant latency offsets across ascending stages.” However, these intracranial data from non-human primate also provide examples of simultaneous onset latencies across the visual hierarchy.

We consider each of these citations in turn and then review other relevant work. Three of the cited publications did not address striate vs. extrastriate latencies. [Givre et al. \(1995\)](#) demonstrated that LGN latencies are shorter than V1 latencies, but did not address timing differences between cortical regions. [Maunsell and Gibson \(1992\)](#) were concerned with changes in V1 responses following LGN lesions and did not record from any other area. [Schroeder et al. \(2004\)](#) is an excellent review detailing how fast multisensory convergence occurs in low-level sensory cortices. However, it does not directly address visual latencies between striate and extrastriate areas. [Raiguel et al. \(1989\)](#) did demonstrate a significant difference in spike latencies with V1 onset occurring before V2 onsets, but “all zones of V5 contained some cells with latencies slightly below those of the most

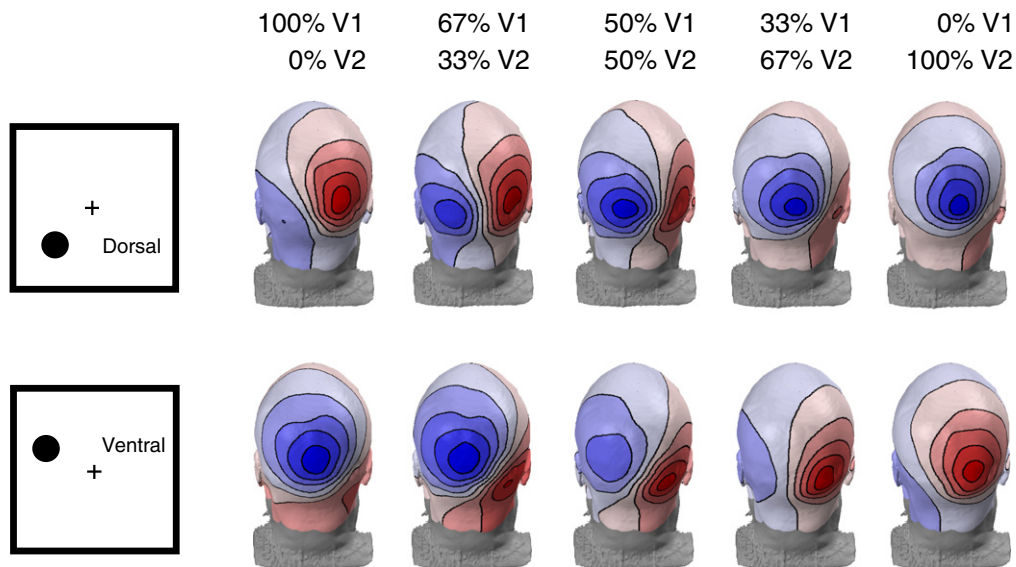


Fig. 3. Scalp topographies for mixtures of V1 and V2. These were simulated using negative activity in both V1 and V2. As in [Fig. 1](#), these are averaged over 10 subjects. Methods for generating these topographies are identical to [Ales et al. \(2010b\)](#). Each color map is scaled separately to highlight the shape of the topography, with red colors representing positive potentials, and blue colors representing negative potentials.

rapid V1 cells” (p. 158). This result demonstrates that V1 is not invariably activated before other visual areas. Nowak et al. (1999) measured the synchronization of spikes between V1 and V2 using V1 spikes occurring anytime after the stimulus to trigger the averaging of V2 responses. They found that V1 and V2 produce synchronized, simultaneous spikes, and discussed, but did not directly address the difference in onset latency following a visual stimulus. An earlier paper from the same group (Nowak et al., 1995) directly addressed onset latencies following visual stimulation and showed that while V1 leads V2 in layer 4, latencies in the supragranular layers of V1 and V2 are the same. The supragranular layers contain pyramidal cells that can contribute strongly to surface potentials (Schroeder et al., 1991). Schmolesky et al. (1998) compared spiking latencies across a wide range of visual areas, and is one of the only studies to include a comparison of V1 and V3. Schmolesky et al. (1998) state:

“The third major finding of the present study is that the dorsal stream signals travel through tiers of the anatomic hierarchy rapidly. Indeed, the fastest layer 4Ca cell encountered exhibited a latency that was only 6 ms longer than the fastest LGNd M cell studied. The average responses of areas V3, MT, MST, and FEF were, in turn, only 6–9 ms longer than the average V1 response.”

These data indicate that only a very brief delay is present between V1 and several dorsal stream cortical areas. Moreover, only 10% of V1 cells had faster latencies than the fastest cells in V2 and V3 (Schmolesky et al., 1998 Fig. 2). Thus, the spike latency distributions of cortical areas largely overlap.

Spike timing vs. transmembrane current measurements

The spike latency data reviewed above do not provide a compelling case for a clear time window for exclusive V1 activity. However, as pointed out by Kelly et al. (this issue), the best intracranial measurements to use for such a comparison are transmembrane current (local field potential) measurements, rather than single neuron spiking latencies, because the former and not the latter are the basis of the surface recorded VEP.

Among the papers cited by Kelly et al. (this issue), the clearest evidence for latency differences between V1 and extrastriate cortex comes from current source density (CSD) recordings in V1 and V2 in response to whole field flash stimuli (Mehta et al., 2000; Schroeder et al., 1998). These studies found large sources in layer 4 of V1 that preceded activity in layer 4 of V2 by about 10 ms. These studies represent some of the best data relating invasively recorded measurements of neural activity to surface ERPs. However, as described in detail below in Sections “How to compare macaques to humans: the 3/5th rule” and “Stimulus differences lead to differences in the laminar activation profile”, stimulus differences make it difficult to draw a direct comparison between latencies measured in different studies. Pattern reversal data for V1 (Schroeder et al., 1991) and for V2 (Schroeder et al., 1998) using stimuli without large luminance transients are available and relevant to interpreting human ERPs, but a specific analysis of latency differences between areas was not provided in these studies and from the data presented it is difficult to determine whether or not there is a difference.

Givre et al. (1994) provides a convincing demonstration that spike latencies are not always directly relevant for predicting current-flow latencies. In macaque V4, Givre et al. (1994) found that “the only action potential correlate that we have observed for the N40 laminar VEP and CSD profiles is a slight reduction in MUA”. Here we have a case of transmembrane currents that could give rise to scalp potentials whose latency would not be reflected in the spike-latencies. In addition, this study provides clear evidence for the simultaneous

activation of V1 and V4 and the contribution of both to the initial surface N40. Givre et al. (1994) state that:

“the mean onset latency of the earliest current sink in the main thalamo-recipient lamina of V1 precedes the earliest sink in V4 by only 2.8 msec”. Furthermore, Givre et al. (1994) found that between V1 and V4 “there was extensive overlap in the distributions with no significant difference in onset latency between areas for two of the three subjects. This similarity of onset latencies can also be seen in the AVREC waveforms for V1 and V4 illustrated in Fig. 5(B)”.

These results show that V4, an area lying well beyond V1 in the cortical hierarchy, has only a negligible latency offset. However, in contrast to Givre et al. (1994), both Schroeder et al. (1998) and a later study (Chen et al., 2007) found that the V4 latency was about 8 ms slower than V1. Despite the discrepancy in the response latency of V4, both of these studies found that responses in V1 and the interparietal sulcus (IP) have the same onset latency. Interestingly, the supragranular layers of V1 and V4 had the same onset latency (See Fig. 5 Chen et al., 2007). Further, latencies in MT were faster than V1 latencies (Fig. 3 Chen et al., 2007). All of the results described above provide evidence for the existence of stages beyond V1 that do not have a latency offset.

There are substantial gaps in our knowledge of response latencies across the brain. Importantly, we have little knowledge of latencies in V3. Compared to macaques, humans have a substantially larger V3 (Van Essen, 2004), nearly as large as V2 (Dougherty et al., 2003). In our simulations, both area V2 and V3 contribute polarity-inverting responses to upper and lower field stimuli. In all of the studies reviewed above, only Schmolesky et al. (1998) contains relevant latency data from V3. This study also contains latency data from MT, which may be instructive here regarding V3. Local field potential data from awake macaque (Chen et al., 2007) show that MT has faster CSD latencies than V1. Schmolesky et al. (1998) found that single units in V3 and MT have nearly identical onset latency distributions. If there is a correlation between spike latency and field potential latency, then V3 could have similar response latency to V1. This raises the possibility that V3 contributes to the earliest parts of C1. But, as noted above, the single unit data from anesthetized macaque may not be directly predictive of VEP recordings. Clearly, this is an important open question that deserves future study.

How to compare macaques to humans: the 3/5th rule

Kelly et al. (this issue) claim that a 3/5th-scaling rule can be used to translate timings between human and non-human primates. The point being that a given latency difference measured in non-human primates should be scaled up by this factor to predict the duration of isolated V1 activity. This conversion factor is derived from Schroeder et al. (1991), Schroeder et al. (1998), and Schroeder et al. (2004). Schroeder et al. (1998) used a diffuse flash of light subtending 20° (26 ms onset latency in V1), while Clark et al. (1995) used a much smaller flashed checkerboard (C1 onset latency was 40–45 ms). While the ratio between 40 and 26 ms is 3/5, because of the difference in stimuli between the two experiments this is not the correct comparison. If we make comparisons between responses to similar stimuli, a much different picture emerges. For flash stimuli recorded at the scalp in humans, the first detectable response occurs at 30 ms (Odom et al., 2009). More compellingly, Ducati et al. (1988) studied the diffuse flash VEP response in humans undergoing thalamotomies using penetrating electrodes inside striate cortex. Ducati et al. (1988) found that the initial latency of responses in striate cortex was 30 ms (peaking around 50 ms). Flash onset latencies are thus very similar across species. For pattern reversal stimuli, Schroeder et al. (1991) suggest that the simian N50 is the same component as the

human N70 (and the P60 is the same as P100 component). However, when measurements are made in humans with subdural electrodes placed on calcarine cortex, the first response for pattern reversal stimuli is between 45 and 55 milliseconds (Farrell et al., 2007), again the same as has been reported for macaque. Because similar intracranial latencies are measured in human and non-human primate when the same stimuli are used, it is questionable that a 3/5th-scaling rule is globally applicable. Finally, it is difficult to choose the correct peak correspondence for scalp components because by the time potentials are measured at the scalp, they reflect the sum of several cortical areas and peak latencies can be shifted by this superimposition.

Stimulus differences lead to differences in the laminar activation profile

Pattern stimuli without luminance transients evoke a very different VEP than a diffuse flash (Odom et al., 2009). While, Clark et al. (1995) used a pattern onset stimulus that also included a luminance increase, many studies of human VEPs have used stimuli that do not include a luminance transient. Schroeder et al. (1991) found that pattern reversal stimuli produced “massive early” activation of the supragranular layers of V1. Schroeder et al. (1991) found that the first reliable component of the surface VEP to pattern reversal was the P60, which arose from “di- and/or trisynaptic activation of supragranular neurons.” Schroeder et al.’s (1991) finding that supragranular neurons generated the first reliable surface VEP is important because the single unit study of (Nowak et al., 1995) found that the latencies in the supragranular layers of V1 and V2 are the same. Another study (Chen et al., 2007) found similar onset latencies in the supragranular layers across a wide range of areas. More studies that make detailed comparisons between laminar activations and their corresponding surface manifestations using stimuli that are used for human ERP recordings are clearly needed.

The polarity of C1

Kelly et al. (this issue) observe that the polarity of the C1 peak is consistent with intracranial data from non-human primates. Schroeder et al. (1998) demonstrated that, for diffuse flash stimuli, the initial activation in both V1 and V2 elicits current sinks in layer 4, with current sources below. This distribution of current sources and sinks corresponds to a dipole oriented with its negative pole towards the cortical surface.

The polarity as measured on the scalp reflects both the orientation of the generator with respect to the cortical surface and the orientation of the cortical surface with respect to the scalp. The scalp polarity as measured at C1 latencies in humans is consistent with a dipole in V1 with its negative pole towards the cortical surface (Clark et al., 1995). Dipoles of this type located in V2, however, produce opposite polarity maxima on the scalp. Following this reasoning Kelly et al. (this issue) suggest that a negative polarity response on midline channels for a stimulus located in the upper horizontal octant identifies V1. This heuristic does not actually isolate V1. We simulated the scalp distributions for different mixtures of V1 and V2 for small targets presented at the nominally optimal stimulus locations (Fig. 3). As demonstrated by the middle bottom topography (50% V1, 50% V2, ventral) in Fig. 3, the expected negative polarity on midline channels is present for 50/50 mixtures of V1 and V2. It is not until V2 activity was greater than V1 activity that the opposite sign was observed.

Another simple rule for identifying a V1 source on the basis of response polarity would be to declare a response as being generated by V1 if the polarity of the maximum matches the polarity of the predicted scalp maximum. In trying to utilize this rule it must be recognized that responses from V2 will modulate the amplitude of the V1 generated response. A pure V1 source in the lower visual field has a positive polarity maximum (top left topography, 100% V1, 0% V2, Fig. 3). The same visual stimulus evokes a negative scalp

maximum when V2 alone is active (top right topography 0% V1, 100% V2, Fig. 3). Upper visual field stimuli produce the opposite polarity maxima. Importantly, the simulation shows that for an activation that includes a 2:1 V1:V2 mixture (67% V1, 33% V2), the polarity of the maximum potential is still consistent with the V1 polarity, even though V2 is active. When V2 has equal, or greater, activation, the polarity of the maximum potential on the scalp reflects the V2 polarity. Therefore, if we know the polarity of the underlying generators in V1 and V2, we can identify which source provides the stronger activation (by the sign of the maximum). However, knowing only the polarity for each source does not enable the exclusion of a mixture of sources. If there is any ambiguity as to the sign of activation in cortex, then even identifying the strongest generator becomes impossible.

Human source estimation studies, discussed in Section “Retinotopically constrained source estimation”, report source polarities in V2 and V3 that are inconsistent with the findings of Schroeder et al. (1998). While the data from Schroeder et al. (1998) are the current best prediction for the source polarities in V1 and V2, the results do not provide the ground truth data for fully resolving this issue, as the data are from diffuse flash stimuli, and not small pattern stimuli without luminance transients. Finally, for V3, an area as important as V2 for the current discussion, the latency and polarity are not currently known.

Interpreting C1 in human studies

At the time of the C1 peak, multiple generators are active

According to Kelly et al. (this issue), the initial 15 ms of the evoked response is immune from contamination from other sources. This 15 ms window arises, in their view, because non-human primate V1 leads V2 by 10 ms, which then should be scaled by 5/3rd. We have questioned if V2 is the only possible contaminating source, and also if the scaling factor is appropriate. For the sake of argument, let’s assume there is a 15 ms time window when only V1 is active. It is common practice to measure C1 at its peak, as the peak is easier to define than the onset time. The C1 peak is reached about 20 ms after its onset latency (Jeffreys and Axford, 1972a). Therefore, by the time of the C1 peak there are already contributions from other visual areas. Indeed, Foxe and Simpson (2002) make this argument and conclude that the C1 peak includes multiple sources and that only the initial 10–15 ms of activation is immune from extrastriate sources (a time period they dub “C1 early”). Further discussion of the nature of the C1 component can be found in a review by Rauss et al. (2011). In addition, even Clark et al. (1995) assumed multiple generators for C1, as they fit their data with two dipole sources.

Even if one accepts the C1 early approach, a final problem arises from typical filter setting used in C1 research. Low-pass filters have the effect of smoothing data and can distort onset/offset times (Chapter 5, Luck, 2005). It is common practice to use low-pass filters with cut-off frequencies at or below 100 Hz when studying C1. For example, Kelly et al. (2008) low-pass filtered at 45 Hz. Low-pass filters at or below 100 Hz can spread responses over more than 10 ms. High-pass filtering can also change the apparent latency of measured components. The smoothing and distortion of the response depend on both the underlying signal, and the impulse response of the chosen filter. Several recent studies (Acunzo et al., 2012; Rousselet, 2012; Widmann and Schroger, 2012) thoroughly investigate the above-mentioned issues and suggest appropriate filter settings. Those studies suggest using causal filters if onset latencies are important for the experimental question. Typically, non-causal filters are used because they minimize distortion of the underlying waveform. Non-causal filters spread distortion both forward and backward in time distorting latency measures. In contrast, causal filters, create more overall waveform distortion but better preserve latency information. Any researcher who wishes to measure the initial 10–15 ms of activation must employ careful

filtering so as not to contaminate this time period with later-generated activity.

Retinotopically constrained source estimation

Kelly et al. claim that the finding of simultaneously-onsetting opposite polarity V1 and V2 sources in Ales et al. (2010a) is not consistent with other data. We agree with Kelly et al. that it is important to take such discrepancies seriously. First, it should be noted that the result Ales et al. (2010a) is consistent with the findings of three other studies that have used retinotopic mapping from fMRI to simultaneously estimate time-courses coming from multiple stimulus locations (Hagler and Dale, 2011; Hagler et al., 2009; Vanni et al., 2004). Each of these studies found a waveform from V1 with its first peak being negative. Each of the studies has also found activity in extrastriate areas V2 and/or V3 that simultaneously onsets with V1. Latency differences between striate and extrastriate are only apparent when comparing between peaks of the same polarity (i.e. N1 to N1). Furthermore, these studies also find evidence for initial positive response in extrastriate areas concurrent to the initial negative response in V1. The studies disagreed as to whether the positive peak was from V2 and/or V3, with some studies attributing it to V2 (Ales et al., 2010a; Hagler and Dale, 2011), another to V3 (Hagler et al., 2009) or both V2 and V3 (Vanni et al., 2004). Ales et al. (2010a) only modeled V2 and could not rule out V3 as a contributing source. As can be seen in Fig. 1, and from our previous study (Ales et al., 2010b), V2 and V3 present very similar topographies, and therefore differentiating between V2 and V3 is difficult for these constrained source localization procedures. Differentiating between V1, V2 and V3 is a difficult due to the proximity of these sources. The existing source localization results, while promising, are still preliminary given the small number of participants that have been studies. Although the resulting responses are similar, each of the studies used very similar techniques and so they cannot be considered to be truly independent as they may share common sources of systematic error. These techniques rely on being able to predict the topography for many different retinotopic locations. Errors in creating the topographic predictions can come from several sources. The electrical model may not be completely accurate (i.e. from not modeling anisotropic conductivity). Retinotopic data from fMRI also is another source of error. Retinotopic maps from fMRI may have local errors (i.e. from draining veins). In addition, obtaining highly accurate alignment of fMRI data with anatomic models is difficult because of distortions in the fMRI data caused B0-susceptibility and gradient nonlinearities.

Direct comparison between the responses from non-human primate data is not possible at present, because of confounding stimulus differences. The retinotopically constrained source estimation studies have either used pattern appearance from a gray background with the same mean luminance (Hagler and Dale, 2011; Hagler et al., 2009; Vanni et al., 2004) or pattern reversal (Ales et al., 2010a). Further, Ales et al. (2010a) used a dense multifocal stimulus that does not result in the same response as standard pattern reversal (Fortune and Hood, 2003). In order to more fully utilize the existing intracranial non-human primate data it is important for a future study using retinotopically constrained source estimation to employ non-patterned luminance increment stimuli. Using stimuli that are more comparable across studies and preparations will enable better validation and improvements for these methods.

Despite the existence of these modeling errors, source localization can be accurate. A recent study (Brodbeck et al., 2011) looked at the surgical outcomes of individuals with epilepsy, determining how accurately EEG source localization predicted the tissue to be resected. The study found that source localization had a sensitivity and specificity that exceeded MRI, PET or SPECT (84% and 88%, respectively). This result demonstrates that source localization can be highly accurate.

While that study was asking a very different question than we address here, it is nevertheless informative as it is one of a very few source localization studies in humans that is able to compare results with strong ground-truth data. As Kelly et al. (this issue) correctly point out, the lack of ground-truth data makes evaluating claims as to the cortical locus generating ERPs is difficult. Continued research on improving methods for recovering sources of ERPs should strive for the best ground-truth comparisons available.

Conclusion

We reiterate that there is no strong evidence that polarity inversion between upper and lower visual field stimuli provides a means to isolate a pure V1 source. We simulated responses from the stimulus locations suggested to produce polarity inversion from V1 sources. The critical stimulus placement failed to create a polarity-inverting source in V1, while V2 and V3 sources still produced polarity inversions. The critical stimulus locations were motivated by a prior study (Clark et al., 1995) that suggested the horizontal meridian was not located at the fundus of the calcarine sulcus. We reviewed anatomical evidence that is inconsistent with this revision of the location of the horizontal meridian. Beyond the anatomical data, we reviewed the functional evidence in both non-human primate and humans for the simultaneous onsetting of several regions outside of V1. We also explained how the 3/5th macaque/human latency conversion factor is questionable because it was based on the comparison of non-corresponding stimuli, and intracranial peak latencies with scalp peak latencies. We discussed human data suggesting multiple sources are active at the peak of C1. Finally, we brought up a technical issue regarding the confounding effects that low-pass filtering can have on estimating onset latencies.

We are not arguing that V1 does not contribute to C1. We are arguing instead that the evidence for C1 being invariably indicative of pure striate activation is not dispositive. It is likely that multiple early visual areas are active during C1. Because extrastriate areas V2 and V3 produce polarity inversions for upper and lower visual fields, there is currently no simple method based on scalp topography for ensuring that V1 is the sole source of activation for an arbitrary stimulus.

References

- Acunzo, D.J., Mackenzie, G., van Rossum, M.C., 2012. Systematic biases in early ERP and ERF components as a result of high-pass filtering. *J. Neurosci. Methods* 209, 212–218.
- Aine, C.J., Suppek, S., George, J.S., Ranken, D., Lewine, J., Sanders, J., Best, E., Tietz, W., Flynn, E.R., Wood, C.C., 1996. Retinotopic organization of human visual cortex: departures from the classical model. *Cereb. Cortex* 6, 354–361.
- Ales, J.M., Carney, T., Klein, S.A., 2010a. The folding fingerprint of visual cortex reveals the timing of human V1 and V2. *Neuroimage* 49, 2494–2502.
- Ales, J.M., Yates, J.L., Norcia, A.M., 2010b. V1 is not uniquely identified by polarity reversals of responses to upper and lower visual field stimuli. *Neuroimage* 52, 1401–1409.
- Bridge, H., Clare, S., Jenkinson, M., Jezzard, P., Parker, A.J., Matthews, P.M., 2005. Independent anatomical and functional measures of the V1/V2 boundary in human visual cortex. *J. Vis.* 5, 93–102.
- Brodbeck, V., Spinelli, L., Lascano, A.M., Wissmeier, M., Vargas, M.L., Vulliemoz, S., Pollo, C., Schaller, K., Michel, C.M., Seeck, M., 2011. Electroencephalographic source imaging: a prospective study of 152 operated epileptic patients. *Brain* 134, 2887–2897.
- Chen, C.M., Lakatos, P., Shah, A.S., Mehta, A.D., Givre, S.J., Javitt, D.C., Schroeder, C.E., 2007. Functional anatomy and interaction of fast and slow visual pathways in macaque monkeys. *Cereb. Cortex* 17, 1561–1569.
- Clark, V.P., Fan, S., Hillyard, S.A., 1995. Identification of early visual evoked potential generators by retinotopic and topographic analyses. *Hum. Brain Mapp.* 2, 170–187.
- Di Russo, F., Martinez, A., Sereno, M.I., Pitzalis, S., Hillyard, S.A., 2002. Cortical sources of the early components of the visual evoked potential. *Hum. Brain Mapp.* 15, 95–111.
- Di Russo, F., Pitzalis, S., Spatoni, G., Aprile, T., Patria, F., Spinelli, D., Hillyard, S.A., 2005. Identification of the neural sources of the pattern-reversal VEP. *Neuroimage* 24, 874–886.
- Dougherty, R.F., Koch, V.M., Brewer, A.A., Fischer, B., Modersitzki, J., Wandell, B.A., 2003. Visual field representations and locations of visual areas V1/2/3 in human visual cortex. *J. Vis.* 3, 586–598.

- Ducati, A., Fava, E., Motti, E.D., 1988. Neuronal generators of the visual evoked potentials: intracerebral recording in awake humans. *Electroencephalogr. Clin. Neurophysiol.* 71, 89–99.
- Farrell, D.F., Leeman, S., Ojemann, G.A., 2007. Study of the human visual cortex: direct cortical evoked potentials and stimulation. *J. Clin. Neurophysiol.* 24, 1–10.
- Fischl, B., Rajendran, N., Busa, E., Augustinack, J., Hinds, O., Yeo, B.T., Mohlberg, H., Amunts, K., Zilles, K., 2008. Cortical folding patterns and predicting cytoarchitecture. *Cereb. Cortex* 18, 1973–1980.
- Fortune, B., Hood, D.C., 2003. Conventional pattern-reversal VEPs are not equivalent to summed multifocal VEPs. *Invest. Ophthalmol. Vis. Sci.* 44, 1364–1375.
- Foxe, J.J., Simpson, G.V., 2002. Flow of activation from V1 to frontal cortex in humans. A framework for defining “early” visual processing. *Exp. Brain Res.* 142, 139–150.
- Galetta, S.L., Grossman, R.L., 2000. The representation of the horizontal meridian in the primary visual cortex. *J. Neuroophthalmol.* 20, 89–91.
- Givre, S.J., Schroeder, C.E., Arezzo, J.C., 1994. Contribution of extrastriate area V4 to the surface-recorded flash VEP in the awake macaque. *Vision Res.* 34 (4), 415–428.
- Givre, S.J., Arezzo, J.C., Schroeder, C.E., 1995. Effects of wavelength on the timing and laminar distribution of illuminance-evoked activity in macaque V1. *Vis. Neurosci.* 12, 229–239.
- Gray, L.G., Galetta, S.L., Schatz, N.J., 1998. Vertical and horizontal meridian sparing in occipital lobe homonymous hemianopias. *Neurology* 50, 1170–1173.
- Hagler Jr., D.J., Dale, A.M., 2011. Improved method for retinotopy constrained source estimation of visual-evoked responses. *Hum. Brain Mapp.* <http://dx.doi.org/10.1002/hbm.21461>.
- Hagler Jr., D.J., Halgren, E., Martinez, A., Huang, M., Hillyard, S.A., Dale, A.M., 2009. Source estimates for MEG/EEG visual evoked responses constrained by multiple, retinotopically-mapped stimulus locations. *Hum. Brain Mapp.* 30, 1290–1309.
- Hinds, O., Polimeni, J.R., Rajendran, N., Balasubramanian, M., Wald, L.L., Augustinack, J.C., Wiggins, G., Rosas, H.D., Fischl, B., Schwartz, E.L., 2008a. The intrinsic shape of human and macaque primary visual cortex. *Cereb. Cortex* 18, 2586–2595.
- Hinds, O.P., Rajendran, N., Polimeni, J.R., Augustinack, J.C., Wiggins, G., Wald, L.L., Diana Rosas, H., Potthast, A., Schwartz, E.L., Fischl, B., 2008b. Accurate prediction of V1 location from cortical folds in a surface coordinate system. *Neuroimage* 39, 1585–1599.
- Holmes, G., 1945. Ferrier lecture: the organization of the visual cortex in man. *Proc. R. Soc. Lond. B Biol. Sci.* 132, 348–361.
- Horton, J.C., Hoyt, W.F., 1991. The representation of the visual field in human striate cortex. A revision of the classic Holmes map. *Arch. Ophthalmol.* 109, 816–824.
- James, A.C., 2003. The pattern-pulse multifocal visual evoked potential. *Invest. Ophthalmol. Vis. Sci.* 44, 879–890.
- Jeffreys, D.A., 1969. Characteristics of visual and auditory evoked potentials. *Neurosci. Res. Program Bull.* 7, 205–227.
- Jeffreys, D.A., 1971. Cortical source locations of pattern-related visual evoked potentials recorded from the human scalp. *Nature* 229, 502–504.
- Jeffreys, D.A., Axford, J.G., 1972a. Source locations of pattern-specific components of human visual evoked potentials. I. Component of striate cortical origin. *Exp. Brain Res.* 16, 1–21.
- Jeffreys, D.A., Axford, J.G., 1972b. Source locations of pattern-specific components of human visual evoked potentials. II. Component of extrastriate cortical origin. *Exp. Brain Res.* 16, 22–40.
- Kelly, S.P., Gomez-Ramirez, M., Foxe, J.J., 2008. Spatial attention modulates initial afferent activity in human primary visual cortex. *Cereb. Cortex* 18, 2629–2636.
- Kelly, S.P., Schroeder, C.E., Lalor, E.C., this issue. What does polarity inversion of extrastriate activity tell us about striate contributions to the early VEP? A comment on Ales et al. (2010). *Neuroimage*. <http://dx.doi.org/10.1016/j.neuroimage.2012.03.081>.
- Luck, S.J., 2005. An introduction to the event-related potential technique. MIT Press, Cambridge, Mass.
- Maunsell, J.H., Gibson, J.R., 1992. Visual response latencies in striate cortex of the macaque monkey. *J. Neurophysiol.* 68, 1332–1344.
- McFadzean, R.M., Hadley, D.M., 1997. Homonymous quadrantanopia respecting the horizontal meridian. A feature of striate and extrastriate cortical disease. *Neurology* 49, 1741–1746.
- McFadzean, R., Brosnahan, D., Hadley, D., Mutlukan, E., 1994. Representation of the visual field in the occipital striate cortex. *Br. J. Ophthalmol.* 78, 185–190.
- Mehta, A.D., Ulbert, I., Schroeder, C.E., 2000. Intermodal selective attention in monkeys. I: distribution and timing of effects across visual areas. *Cereb. Cortex* 10, 343–358.
- Nowak, L.G., Munk, M.H., Girard, P., Bullier, J., 1995. Visual latencies in areas V1 and V2 of the macaque monkey. *Vis. Neurosci.* 12, 371–384.
- Nowak, L.G., Munk, M.H., James, A.C., Girard, P., Bullier, J., 1999. Cross-correlation study of the temporal interactions between areas V1 and V2 of the macaque monkey. *J. Neurophysiol.* 81, 1057–1074.
- Odom, J.V., Bach, M., Brigell, M., Holder, G.E., McCulloch, D.L., Tormene, A.P., Vaegan, 2009. ISCEV standard for clinical visual evoked potentials (2009 update). *Doc. Ophthalmol.* 120, 111–119.
- Raiguel, S.E., Lagae, L., Gulyas, B., Orban, G.A., 1989. Response latencies of visual cells in macaque areas V1, V2 and V5. *Brain Res.* 493, 155–159.
- Rajimehr, R., Tootell, R.B., 2009. Does retinotopy influence cortical folding in primate visual cortex? *J. Neurosci.* 29, 11149–11152.
- Rauss, K., Schwartz, S., Pourtois, G., 2011. Top-down effects on early visual processing in humans: a predictive coding framework. *Neurosci. Biobehav. Rev.* 35, 1237–1253.
- Rousselet, G.A., 2012. Does filtering preclude us from studying ERP time-courses? *Front. Psychol.* 3, 131.
- Schmolesky, M.T., Wang, Y., Hanes, D.P., Thompson, K.G., Leutgeb, S., Schall, J.D., Leventhal, A.G., 1998. Signal timing across the macaque visual system. *J. Neurophysiol.* 79, 3272–3278.
- Schroeder, C.E., Tenke, C.E., Givre, S.J., Arezzo, J.C., Vaughan Jr., H.G., 1991. Striate cortical contribution to the surface-recorded pattern-reversal VEP in the alert monkey. *Vision Res.* 31, 1143–1157.
- Schroeder, C.E., Tenke, C.E., Givre, S.J., 1992. Subcortical contributions to the surface-recorded flash-VEP in the awake macaque. *Electroencephalogr. Clin. Neurophysiol.* 84, 219–231.
- Schroeder, C.E., Mehta, A.D., Givre, S.J., 1998. A spatiotemporal profile of visual system activation revealed by current source density analysis in the awake macaque. *Cereb. Cortex* 8, 575–592.
- Schroeder, C., Molholm, S., Lakatos, P., Ritter, W., Foxe, J., 2004. Humansimian correspondence in the early cortical processing of multisensory cues. *Cogn. Process.* 5, 140–151.
- Slotnick, S.D., Klein, S.A., Carney, T., Sutter, E., Dastmalchi, S., 1999. Using multi-stimulus VEP source localization to obtain a retinotopic map of human primary visual cortex. *Clin. Neurophysiol.* 110, 1793–1800.
- Spalding, J.M., 1952. Wounds of the visual pathway. Part II. The striate cortex. *J. Neurol. Neurosurg. Psychiatry* 15, 169–183.
- Stensaas, S.S., Eddington, D.K., Dobelle, W.H., 1974. The topography and variability of the primary visual cortex in man. *J. Neurosurg.* 40, 747–755.
- Van Essen, D.C., 1997. A tension-based theory of morphogenesis and compact wiring in the central nervous system. *Nature* 385, 313–318.
- Van Essen, D., 2004. Organization of visual areas in macaque and human cerebral cortex. In: Werner, J.S., Chalupa, L.M. (Eds.), *The Visual Neurosciences*. MIT Press, Cambridge, Mass.
- Vanni, S., Warnking, J., Dojat, M., Delon-Martin, C., Bullier, J., Segebarth, C., 2004. Sequence of pattern onset responses in the human visual areas: an fMRI constrained VEP source analysis. *Neuroimage* 21, 801–817.
- Widmann, A., Schroger, E., 2012. Filter effects and filter artifacts in the analysis of electrophysiological data. *Front. Psychol.* 3, 233.
- Wilms, M., Eickhoff, S.B., Homke, L., Rottschy, C., Kujovic, M., Amunts, K., Fink, G.R., 2010. Comparison of functional and cytoarchitectonic maps of human visual areas V1, V2, V3d, V3v, and V4(v). *Neuroimage* 49, 1171–1179.
- Zhang, X., Hood, D.C., 2004. A principal component analysis of multifocal pattern reversal VEP. *J. Vis.* 4, 32–43.